

# Imaging features of alveolar soft part sarcoma\*

Teng Jin<sup>1</sup>, Ping Zhang (Co-first author)<sup>2</sup>, Xiaoming Li<sup>3</sup> (✉)

<sup>1</sup> Department of Radiology, Renmin Hospital of Wuhan University, Wuhan 430060, China

<sup>2</sup> Department of Radiology, The Third Hospital of Hebei Medical University, Shijiazhuang 050051, China

<sup>3</sup> Department of Radiology, Tongji Hospital, Tongji Medical College, Huazhong University of Science and Technology, Wuhan 430030, China

## Abstract

**Objective** The aim of this study was to analyze the imaging features of alveolar soft part sarcoma (ASPS).

**Methods** The imaging features of 11 cases with ASPS were retrospectively analyzed.

**Results** ASPS mainly exhibited an isointense or slightly high signal intensity on T1-weighted imaging (T1WI), and a mixed high signal on T2-weighted imaging (T2WI). ASPS was partial, with rich tortuous flow voids, or “line-like” low signal septa. The essence of the mass was heterogeneous enhancement. The 1H-MRS showed a slight choline peak at 3.2 ppm.

**Conclusion** The well-circumscribed mass and blood voids, combined with “line-like” low signals play a significant role in diagnosis. The choline peak and the other signs may be auxiliary diagnoses.

**Key words:** alveolar soft part sarcoma (ASPS); imaging features; clinical findings

Received: 18 June 2015  
Revised: 12 July 2015  
Accepted: 25 July 2015

Alveolar soft part sarcoma (ASPS) is a rare tumor, accounting for 0.5%–0.9% of all soft-tissue sarcomas in adults. ASPS accounts for 0.8–1.8% of all tumors found in children <sup>[1]</sup>, and is commonly seen in young females <sup>[2]</sup>. This type of tumor has two predilection sites: the lower extremities in adults and the head and neck region in infants and children <sup>[3]</sup>. The tumor is rich in vascular tissue, and is almost asymptomatic during the early stages; therefore, metastasis may be a relative characteristic of the tumor. ASPS frequently metastasizes to the lungs (42%), bones (19%), brain (15%), and lymph nodes (7%) <sup>[4]</sup>. ASPS typically shows a high signal intensity in T1-weighted imaging (T1WI) and T2-weighted imaging (T2WI). The images of this tumor are rich in intra- and extra-tumoral vascular flow void signals; therefore, this may be a specific manifestation of this tumor <sup>[5]</sup>. As it is a rare disease, a majority of the references on ASPS are case reports; therefore, the features of dynamic contrast-enhanced magnetic resonance imaging (DCE-MRI) and 1H-MR spectroscopy (1H-MRS) in ASPS have been rarely observed in previous studies. In this study, the MRI features of 11 patients with ASPS were analyzed, in an attempt to improve the levels of ASPS diagnosis.

## Materials and methods

### Clinical data

Eleven patients (6 males, 5 females; age range, 21–62 years; mean age, 32 years) with ASPS, proved by histopathological examinations between January 2007 and March 2014, were retrospectively reviewed. Six of these patients were under 30 years, and 9 were aged below 40. An institutional review board exemption and waiver for the requirement of written informed consent was obtained for this retrospective study. A majority of the patients sought medical care for a painless mass, or a mass found accidentally by physical examination (7/11); one of these patients sought treatment for a headache (1/11). Based on palpation, it was classified as a single, firm, non-tender mass (6/11).

### Medical imaging

The equipment used in this study included a 3.0T MR scanner (Syngo MRD13; Siemens, Germany), a 1.5T MR scanner (Signa HDxt; GE Healthcare, USA), and a CT scanner (Discovery 750 HD CT; GE Healthcare, USA). All 11 patients were subjected to conventional MRI. Five

✉ Correspondence to: Xiaoming Li. Email: lilyboston2002@163.com

\* Supported by a grant from the National Scientific foundation of China (No. 81320108013, 31170899).

© 2015 Huazhong University of Science and Technology

**Table 1** Clinical characteristics and MRI features of patients with ASPS

No.	Sex	Age (years)	Clinical features	Imaging features			1H-MRS
				T1WI	T2WI	Contrast enhanced MRI	
1	Female	42	A spherical painless mass in left hip	Iso-signal	High signal with "line-like" low signal and flow voids	–	–
2	Male	21	A spherical painless mass in right hip	Iso-signal	High signal with "line-like" low signal and flow voids	–	–
3	Female	22	A spherical painless mass in abdominal wall	Iso-signal	High signal with "line-like" low signal and flow voids	–	–
4	Male	27	A sacrococcygeal round painless mass	Iso-signal	High signal with "line-like" low signal and flow voids	arteries surround the mass	choline peak rise
5	Female	21	A oval painless mass in fossa iliaca	Iso-signal	High signal with "line-like" low signal and flow voids	tortuous vessels enhanced	choline peak rise
6	Male	62	Multiple masses in fossa iliaca	high-signal	High signal with "line-like" low signal and flow voids	–	–
7	Female	25	A round pain mass in left thigh	Iso-signal	High signal with "line-like" low signal and flow voids	tortuous vessels enhanced	–
8	Male	33	A stiff painless mass in left superficial thigh	Iso-signal	High signal with "line-like" low signal and flow voids	–	–
9	Male	34	A painless mass in right arm	Iso-signal	High signal with "line-like" low signal	–	–
10	Female	28	A fusiform pain mass in right arm	Iso-signal	High signal	–	–
11	Male	38	Headache with irregular pain mass in right orbit	Iso-signal	High signal	tortuous vessels enhanced	choline peak rise

patients were subjected to contrast-enhanced MRI, and one patient to DCE-MRI DCE-MRI, utilizing the TWIST sequence, MRS, and spiral CT angiography (CTA). One patient underwent a 1H-MRS and a spiral CTA examination each.

Two musculoskeletal radiologists (fifteen years of work experience), who were blinded to the diagnosis and the disease history of patients, were requested to evaluate the masses based on a consensus; this included an analysis of the location, signal, shape, boundary, size, enhancement, and spectrum.

Two pathologists with more than sixteen years of work experience, who were blinded to the disease history of the patients, were asked to evaluate all of the stained slides based on a consensus.

## Results

### Tumor location

There were no significant traits in the location of ASPS. The tumors were located in the hip (2 cases); regions adjacent to the hip (5 cases), including the sacrococcygeal region (1 case), left iliac fossa (1 case), right iliac bone (1 case), low abdominal wall (1 case), and the root of thigh (1 case); and in the extremities, including the arm (2 case), thigh (1 case), and the orbit (1 case).

### Tumor size

The size of the ASPS tumor was usually large, with the length-diameter ranging from 34 mm to 92 mm (average, 62.4 mm). The largest mass was located in the sacrococcygeal region, while the smallest was situated in the orbit.

### Tumor shape and border

The tumors were sphere-shaped (9/11) or fusiform (1/11). The boundaries of ASPS ranged from relatively clear (9/11) to unclear (2/11). Four of the patients showed bone erosions. Metastasis was seen in 7 patients (4 in the lung, 1 in the brain, 2 in the lymph nodes).

### Characteristics of the MRI and CT scan images

ASPS showed a high or iso-signal intensity on T1WI (Fig. 1a, Fig. 2a) and a high-intensity on T2WI (Fig. 1b, Fig. 1c and Fig. 2b), relative to the muscle (11/11). Four cases displayed regions with multiple necrosis (Fig. 1d) and one showed a hemorrhage. Flow voids were observed in 8/11 cases in the core or margin of the tumor (Fig. 1e, Fig. 2b). Multiple "line-like" low signal septa were seen in 9/11 cases (Fig. 2c). Five cases were non-uniformly distributed (5/5) when observed by contrast enhanced MRI, wherein regions of cystoid variation and necrosis were not obviously enhanced. The "line-like" septa were also not enhanced. The DCE-MRI and CTA images of tumors in three patients showed a rich blood supply (Fig. 1f, Fig. 1g, and Fig. 2d). Brain metastasis also showed signal voids

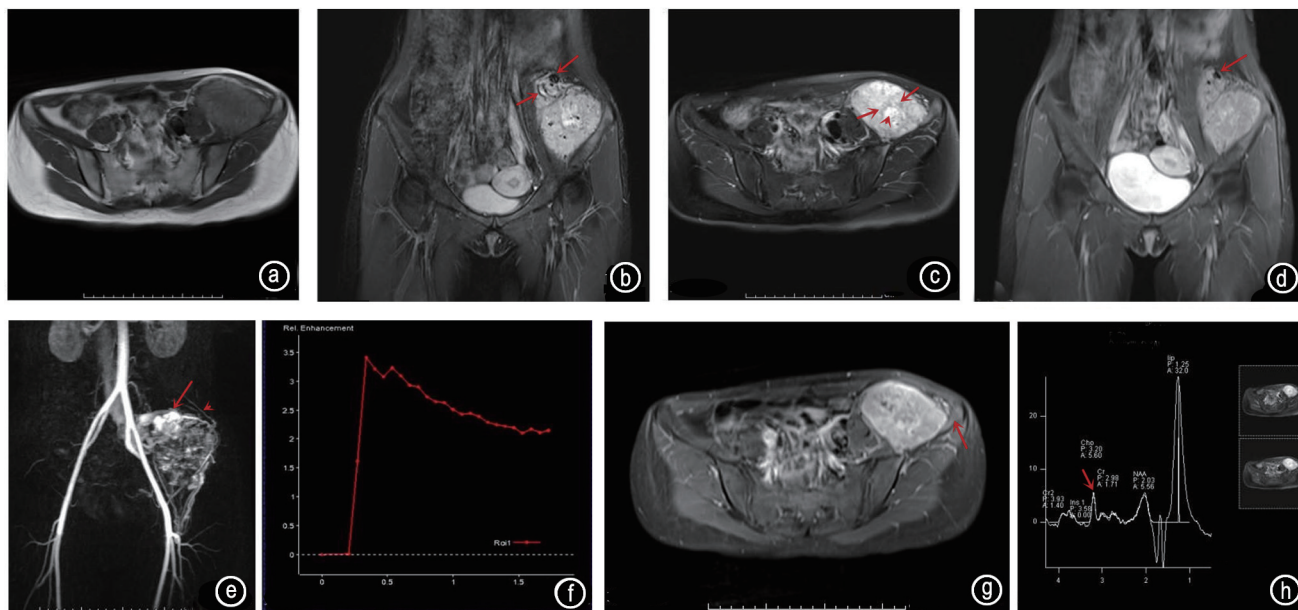


**Fig. 1** A 21-year-old patient with alveolar soft part sarcoma in the left iliac fossa. The mass showed a slightly high signal intensity on T1WI (a) (TR/TE = 766/22 ms). Coronal fat suppression T2WI (b) (TR/TE = 3000/38 ms) showed a round mass, with multiple tortuous flow voids of vessels (arrows), a significantly high intensity on T2WI (c) (TR/TE = 2400/84 ms), with a little necrosis (arrowhead). The tumor was separated by multiple “line-like” low signals (arrow), both on T1WI and T2WI. Coronal contrast-enhanced T1WI (d) (TR/TE = 280/7.2 ms) showed that the tortuous vessels are not enhanced after the injection of contrast medium (Gadovist, 0.1 mmol/kg). The TWIST sequence (e) (TR/TE = 3/1.11 ms, 25 phases) indicated that the tumor was highly vascular, which was supplied by the left external iliac artery and surrounded by dilated veins (arrowhead); the tortuous signal voids of vessels seen on T2WI were essentially thick supplying arteries (arrow). The time-signal intensity curve of DCE-MRI (f) showed the rapid rise during the early stage and the slow eventual descent. (g) The tumor was obviously enhanced, and its adjacent iliac bone was slightly enhanced (arrow). MRS (h) showed a discrete choline peak at 3.2 ppm (arrow). TR: repetition time; TE: echo time

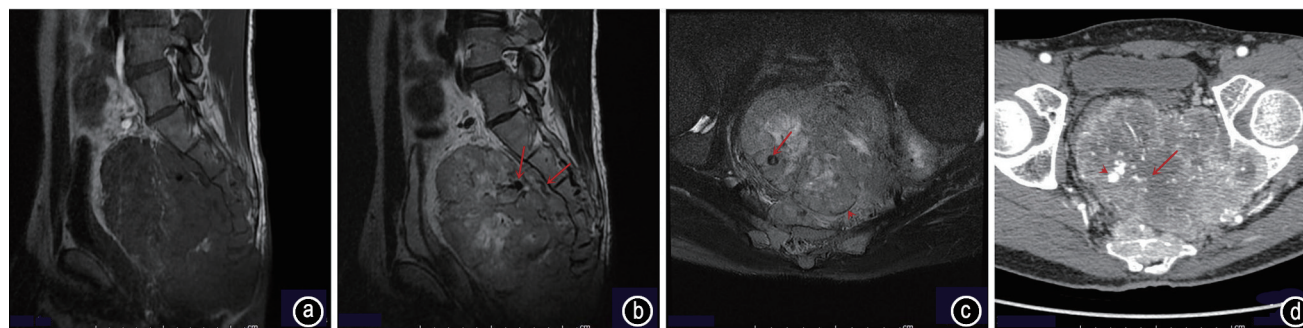


**Fig. 2** A 27-year-old male patient with ASPS. Sagittal T1WI (A) (TR/TE = 340/7.28 ms) showed that the mass is well-defined, and an iso-intensity signal. Multiple signal voids were seen in the mass on sagittal T2WI (B) (TR/TE = 2200/123.75 ms) (arrows). Axial T2WI (c) (TR/TE = 2480/117.72 ms) demonstrated that the mass shows a mixed high signal intensity with multiple “line-like” low signals (arrowheads), the round signal voids (long arrow) and the iso-signal intensity in the center (short arrow). CTA (D) showed dilated supplying arteries throughout, or surrounding the whole mass (arrows) of the necrosis (long arrow) without enhancement. Left acetabulum and sacrum bone were seriously invaded. TR: repetition time; TE: echo time

on MRI; many nodules in lung metastasis were arranged in a snow-like pattern, as observed on the CT scans. The big, twisted supplying arteries corresponded to the vascular flow voids regions in the images obtained by T2-weighted DCE-MRI. The time-signal intensity curve of T2-weighted DCE-MRI indicated a rapid rise in the perfusion of ASPS during the early stages, which decreased

over a subsequent period of time (1/1). 1H MRS imaging revealed a distinct choline peak (Fig. 1h) at 3.2 ppm (2/2; Table 1).

### Histopathological presentation

A photomicrograph of ASPS showed a typical tumor cell aggregation, like a nest or an alveolar structure (Fig.

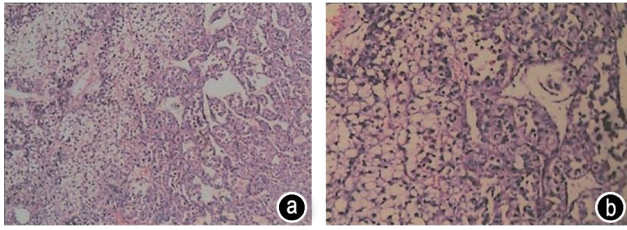


**Fig. 3** Photomicrographs (H&E, ×100). The large and polygonal tumor cells are arranged in solid nests and/or alveolar structures with very large and atypical vesicular nuclei. Necrosis was also observed

3). The cells in the center of the nest were degenerated or undergoing necrosis. Capillary networks and fiber tissues were also observed in the intercellular space. Immunohistochemical analysis revealed that some of the patients were positive for S-100 protein (1/5), vim (1/3), MyoD1 cytoplasm (1/3), and Neuro Specific Enolase (1/1), and negative for other tumor markers.

## Discussion

### Clinical features and pathological features

ASPS is a rare malignant tumor affecting soft tissues, with a peak age of incidence of 15–35 years<sup>[6]</sup>. It can occur in any region of the body, and is commonly found in the extremities or the trunk<sup>[2]</sup>. Our research indicates that the hip and its adjacent anatomic structures are the common locations of the tumor. Even when the tumor occurs in the thigh, it tends to be closer to the hip. Some studies have shown a higher incidence of ASPS on the right side of the body<sup>[7]</sup>. Our research did not reveal any such tendency. ASPS is a slow-growing tumor that is usually painless; therefore, this tumor has been described as a “disease that whispers”, owing to its hypervascularity. Metastasis has been reported in 20–25% of the patients at the time of diagnosis<sup>[8]</sup>. In this study, the lungs were the most common tumor sites, which correlated with the results of a previous report<sup>[9]</sup>. The patients’ median survival rate has been reported to be 48 months, with an overall 5-year survival rate of 38%<sup>[10]</sup>. Tumor cells were arranged in “nest-like” or alveolar structures in all cases. PAS stain was seen to be positive; the rod shape crystal of the PAS stain could significantly assist in differentiating the primary and metastasis ASPS<sup>[11]</sup>.

### Radiological features

Unenhanced T1-weighted MRI of ASPS usually demonstrated an iso-intense or slightly high-intense signal relative to the muscle, while the T2-weighted MRI showed a heterogeneous high signal. Chen *et al*<sup>[8]</sup> attributed the slightly high-intense signal in T1-weighted MRI and the high signal in T2-weighted MRI to the slow flow of blood. Multiple serpentine signal voids within the tu-

mors in all sequences may be a relative characteristic appearing in ASPS. Previous studies have reported that high blood flow leads to such phenomena<sup>[12]</sup>, and that slow blood flow is a certain cause of patch high signal intensity on T2WI. However, it is difficult to separate such a high signal intensity lesions from that for hemorrhage. In this study, 9 cases showed a “line-like” low signal septa on T1-weighted and T2-weighted MRI, due to the fibrous septum between tumor cell nests. The “line-like” substances are fibers; however, such manifestations are not specific, and usually appear in fibrosarcoma. ASPS was heterogeneously well-enhanced by contrast-enhanced CT and MRI owing to its abundant blood supply; the solid portion was rapidly enhanced after the injection of contrast medium. On the other hand, necrosis and “line-like” low signal septa were not enhanced in our study. The DCE-MRI, utilizing the TWIST sequence, clearly showed thick or twisted supplying arteries as flow voids on T2WI. Two cases subjected to CTA scanning displayed winding supply arteries entering the core from the edge of tumor. Venous drainage disorders (displayed on a DCE-MRI) around the tumor could be easily misdiagnosed as arteriovenous malformation<sup>[12–13]</sup>. The time-signal intensity curve showed a rapid rise (30 s), and a relative slow fall, in one case. The specificity of this feature needs further study (as the number of cases in this study is not enough to draw a definitive conclusion). MRS showed a distinct choline peak at 3.2 ppm in two cases. The choline peak reflects the induction of glycerophosphoryl choline and phosphorylcholine, which are involved in the synthesis and breakdown of cell membrane phospholipids. We observed a significant increase in the choline content in malignant tumors, which reflects the increase in cell membrane conversion<sup>[14]</sup>. In addition, our study indicated the appearance of a signal void in brain metastasis on an MRI, as well as many nodules in lung metastasis arranged as snow-like type on CT scans. Some previous studies have<sup>[8]</sup> reported that satellite nodules around the primary lesion may be a specific sign of ASPS; however, according to our statistics, only one-eleventh of the cases showed the attachment of nodules to the mass.

### Differential diagnosis

The differential diagnosis includes vascular malformations and highly vascularized soft tissue tumors<sup>[15]</sup>. Fibrosarcoma, arteriovenous malformations, and hemangioma need to be distinguished from ASPS.

### Myxofibrosarcoma

Fibrosarcoma also shows an iso-signal intensity or slightly high signal intensity in T1WI, and a mixed high signal on T2WI, relative to the muscles<sup>[16]</sup>. However, this tumor is most commonly seen in old people, and occa-

sionally in young adults<sup>[17]</sup>. This tumor usually presents a lobulated shape located in the superficial layer. Its enhancement is homogeneous or heterogeneous. Myxofibrosarcoma has been frequently reported to show curvilinear extensions (which histopathologically represents fascial extension) exhibiting a high T2 signal; in addition, this is enhanced on post-gadolinium MRI<sup>[18]</sup>, which may be a relative specific manifestation that is not shown by ASPS. The signal void feature is not to be found in correlative literature pertaining to myxofibrosarcoma.

### Arteriovenous malformations

Because of the existence of flow voids, ASPS may be misdiagnosed as an arteriovenous malformation; ASPS can be distinguished from arteriovenous malformations by the significant soft tissue component and slow washout of contrast medium. Meanwhile, arteriovenous malformation has exclusive vascular components, with scanty solid-tissue components in the tumor. In addition, hemorrhage is more common in arteriovenous malformations than in ASPS<sup>[11]</sup>.

### Hemangioma

Although hemangioma demonstrates a slightly high-signal-intensity on T1WI, and a “light bulb sign” on T2WI, which indicates that the signal on T2WI of hemangioma may be more homogeneous and higher than that of ASPS. In addition, hemangioma often shows an irregular margin, while ASPS usually presents an oval or round shape. Many other tumors, such as malignant fibrous histiocytoma, metastatic melanoma, and soft-tissue tumor with hemorrhage, may present an iso-intensity signal or a slightly high signal intensity on T1WI; however, signal voids of vessels are not frequently observed in these tumors. The tumor border may be another point allowing for their differentiation.

### Conclusion

The radiological features of ASPS include a round image, with iso- or high signal intensity on T1WI, and a mixed high signal intensity, multiple tortuous flow voids, and a “line-like” low signal. Contrast-enhanced MR or CTA demonstrate thick twisted supply arteries, or multiple regurgitant veins around the tumor. Among the numerous radiological characteristics of ASPS, a well-circumscribed mass and blood voids combined with “line-like” low signal definitely play a significant role in the diagnosis of ASPS. The distinct choline peak in MRS, time-signal intensity curve, satellite nodules, or the other signs may comprise auxiliary diagnoses.

### Conflicts of interest

The authors indicated no potential conflicts of interest.

## References

- Ordóñez NG. Alveolar soft part sarcoma: a review and update. *Adv Anat Pathol*, 1999, 6: 125–39.
- Pennacchioli E, Fiore M, Collini P, *et al.* Alveolar soft part sarcoma: clinical presentation, treatment, and outcome in a series of 33 patients at a single institution. *Ann Surg Oncol*, 2010, 17: 3229–3233.
- Ahn SH, Lee JY, Wang KC, *et al.* Primary alveolar soft part sarcoma arising from the cerebellopontine angle. *Child Nerv Syst*, 2014, 30: 345–350.
- Chen YD, Hsieh MS, Yao MS, *et al.* MRI of alveolar soft-part sarcoma. *Comput Med Imaging Graph*, 2006, 30: 479–482.
- Sidi V, Fragandrea I, Hatzipantelis E, *et al.* Alveolar soft-part sarcoma of the extremity: a case report. *Hippokratia*, 2008, 12: 251–253.
- Lieberman PH, Foote FW Jr, Stewart FW, *et al.* Alveolar soft-part sarcoma. *Jama*, 1966, 198: 1047–1051.
- Lieberman PH, Brennan MF, Kimmel M, *et al.* Alveolar soft-part sarcoma. A clinico-pathologic study of half a century. *Cancer*, 1989, 63: 1–13.
- Pang LM, Roebuck DJ, Griffith JF, *et al.* Alveolar soft-part sarcoma: a rare soft-tissue malignancy with distinctive clinical and radiological features. *Pediatr Radiol*, 2001, 31: 196–199.
- van Ruth S, van Coevorden F, Peterse JL, *et al.* Alveolar soft part sarcoma. a report of 15 cases. *Eur J Cancer*, 2002, 38: 1324–1328.
- Wakely PE Jr, McDermott JE, Ali SZ. Cytopathology of alveolar soft part sarcoma: a report of 10 cases. *Cancer*, 2009, 117: 500–507.
- Suh JS, Cho J, Lee SH, *et al.* Alveolar soft part sarcoma: MR and angiographic findings. *Skeletal radiology*, 2000, 29: 680–689.
- Park MY, Jee WH, Kim SK, *et al.* Preliminary experience using dynamic MRI at 3.0 Tesla for evaluation of soft tissue tumors. *Korean J Radiol*, 2013, 14: 102–109.
- Negendank WG, Sauter R, Brown TR, *et al.* Proton magnetic resonance spectroscopy in patients with glial tumors: a multicenter study. *J Neurosurg*, 1996, 84: 449–458.
- Temple HT, Scully SP, O’Keefe RJ, *et al.* Clinical presentation of alveolar soft-part sarcoma. *Clin Orthop Relat Res*, 1994, 300: 213–218.
- Hashemi A, Tefagh S, Seifadini A, *et al.* Infantile fibrosarcoma in a child: a case report. *Iranian journal of pediatric hematology and oncology*, 2013, 3:135–137.
- Clarke LE, Zhang PJ, Crawford GH, *et al.* Myxofibrosarcoma in the skin. *J Cutan Pathol*, 2008, 35: 935–940.
- Feki S, Frikha F, Ben Hadj Hmida Y, *et al.* Prevalence and diagnostic value of antinuclear antibodies without identified antigenic target: a retrospective study of 90 patients. *Rev Med Interne*, 2012, 33: 475–481.
- Lai YC, Chiou HJ, Wu HT, *et al.* Ultrasonographic and MR findings of alveolar soft part sarcoma. *J Chin Med Assoc*, 2009, 72: 336–339.

DOI 10.1007/s10330-015-0108-6

Cite this article as: Jin T, Zhang P, Li XM. Imaging features of alveolar soft part sarcoma. *Oncol Transl Med*, 2015, 1: 159–163.